

## **Glassy (Al,Fe)<sub>2</sub>O<sub>3</sub> in bauxites from the Southern Highlands of NSW**

**Tony Eggleton<sup>1</sup> and Graham Taylor<sup>2</sup>**

<sup>1</sup>Research School of Earth Sciences, Australian National University, Canberra, ACT.

Email: [Tony.Eggleton@anu.edu.au](mailto:Tony.Eggleton@anu.edu.au)

<sup>2</sup>University of Canberra, Belconnen, ACT.

### **Introduction**

Across the Southern Highlands of New South Wales are sporadic ferruginous bauxites, mostly overlying Eocene basalts (Owen 1954). Abundant throughout these deposits are hard, vitreous, highly magnetic nodules and pisoliths. These yield a weak diffraction pattern and are referred to as containing “Poorly Diffracting Material”, or PDM. This paper describes the properties of this material and discusses its formation.

### **Appearance**

Pisoliths and nodules having a vitreous lustre and conchoidal fracture were selected for this study (Figure 1). Under binocular microscopy they range in colour from transparent pale yellow through increasingly darker and increasingly opaque shades of yellow-brown and brown to black. The colour variation is apparent at scales down to at least 0.1 mm. Black and brown fragments are strongly magnetic, yellow fragments are weakly- or non-magnetic.

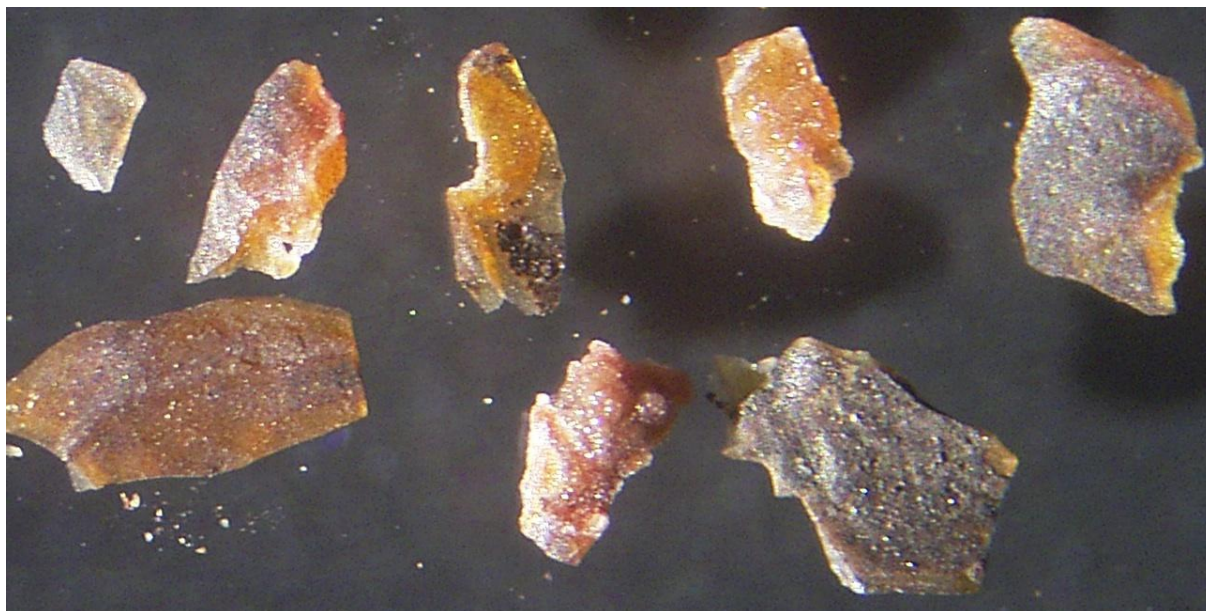


**Fig 1.** Millimetre-sized chips of PDM; ranging in colour from yellow (non magnetic) to dark brown (highly magnetic).

## XRD

The mineralogical composition of the vitreous pisolithic bauxite bulk samples and separated magnetic and non-magnetic fractions are dominated by PDM, with gibbsite, hematite and maghemite as the major minerals. Individual vitreous cores of pisoliths and nodules are very high in PDM (Table 1). The crystal size of the iron minerals is approximately 20 nm (Scherrer equation).

**Table 1.** Mineralogical composition of magnetic vitreous bauxite from Windellama. NSW

	Windellama
PDM	58
Quartz	1
Gibbsite	8
Hematite	18
Maghemite	12
Pseudobrookite	1
Anatase	1
Rutile	1

XRD patterns of PDM show, in addition to the peaks attributable to the minerals listed in Table 1, three broad peaks at 2.41 Å, 2.11 Å and 1.39 Å, and in some instances weaker peaks at 2.84 Å, 1.99 Å and 1.44 Å (Figure 2). These peaks can be matched quite closely to those for  $\chi$ -alumina reported by Brindley & Choe (1961) (Table 2). Figure 2 shows a difference XRD pattern generated by Siroquant after subtraction of peaks from gibbsite, hematite and maghemite. The peak at 4.8 Å may be from PDM, but is more likely residual gibbsite.

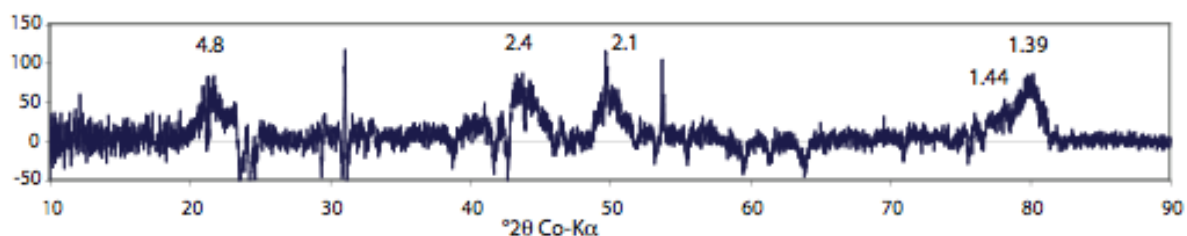


**Fig 2.** Difference XRD scan using Siroquant™ of the non-magnetic fraction of glassy bauxite nodule Tarago 5D after subtraction of gibbsite and hematite. Peak positions in Å.

**Table 2.** Broad peaks in PDM XRD difference patterns compared to the data for  $\chi$ -alumina of Brindley & Choe (1961).

PDM		$\chi$ -alumina (Brindley & Choe 1961)		
I	d	I	d	hkl
If present, obscured by gibbsite		10	4.82	100
weak	2.85	25	2.88	003
strong	2.41	40	2.41	200
medium	2.11	45	2.12	202
weak	1.99	30	1.96	104
weak	1.44	nr	nr	006
strong	1.39	100	1.395	220

### Electron microscopy

PDM in nodules and the cores of pisoliths is complex and particulate at all levels of magnification. PDM with least  $\text{Fe}_2\text{O}_3$  appears fairly uniform under back-scatter electron imaging (Figure 3a), then as the  $\text{Fe}_2\text{O}_3$  content increases, small bright crystals and patches of hematite and maghemite show more abundantly (Fig 3 b - d). Under TEM, PDM resolves into 10 nm crystals (Figure 4).

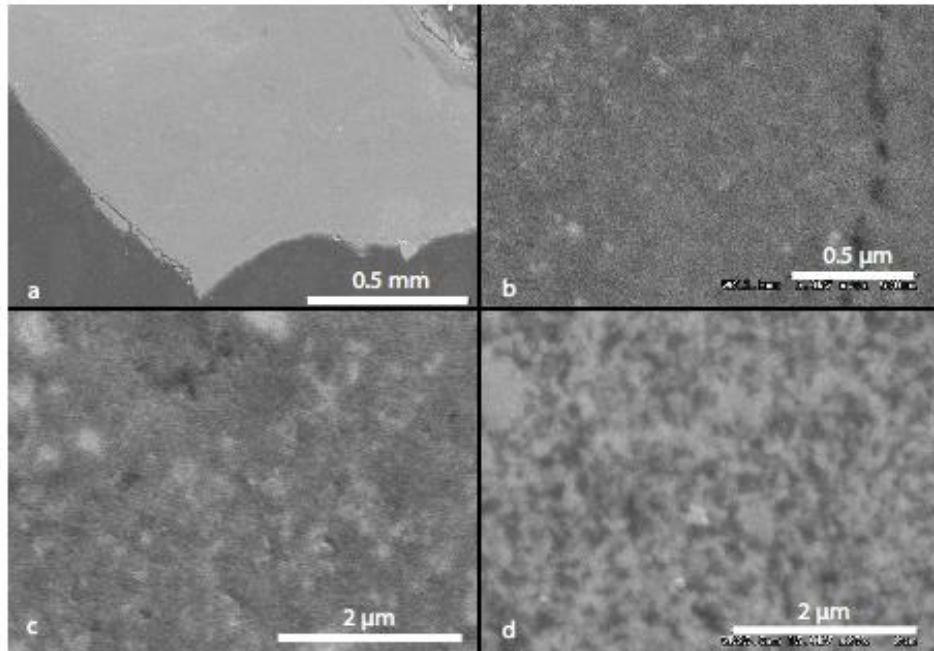


**Fig 3.** Back-scatter SEM images of PDM (a) Low Fe uniform appearing PDM at low magnification. Brightness in (a) is enhanced relative to b), c) and d). (b) PDM with ca 10%  $\text{Fe}_2\text{O}_3$  showing as small white spots. (c) PDM with 30%  $\text{Fe}_2\text{O}_3$ . (d) PDM with ~50%  $\text{Fe}_2\text{O}_3$

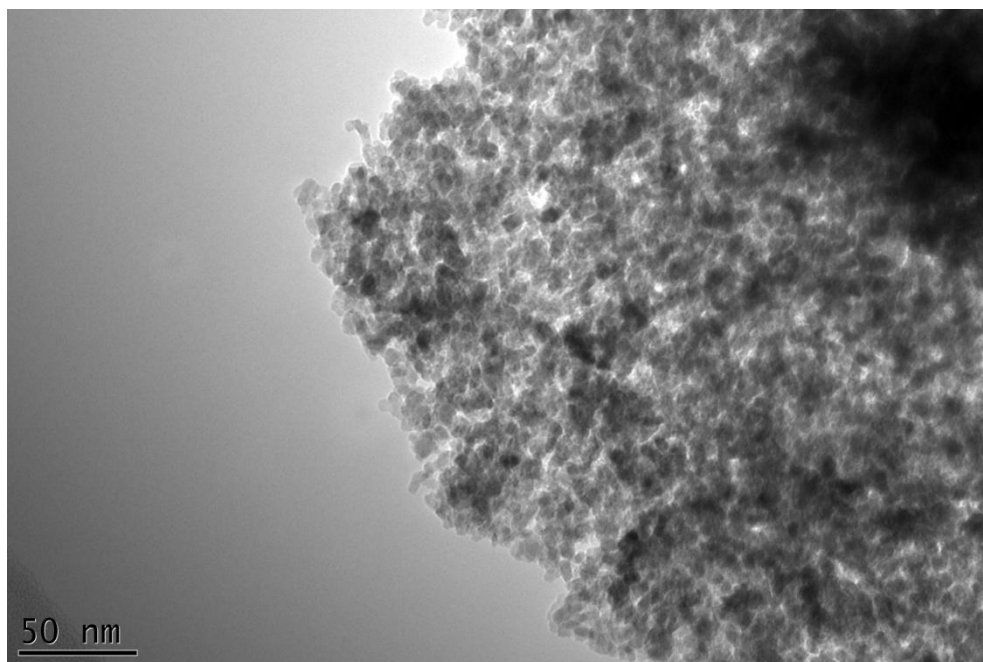


**Fig 4.** TEM image of PDM, showing ~ 10 nm crystals. Sample Windellama 13.

### Composition

The bulk composition of PDM-rich particles in the bauxite is about 90% ( $\text{Al}_2\text{O}_3 + \text{Fe}_2\text{O}_3$ ) with these components varying widely between particles analysed, and appreciably within one pisolith or nodule. An average of three Fe-poor analyses is listed in Table 3. Figure 5 shows the variation in composition, scaled to 100%, based on EMP analyses of many particles from several localities.

Analyses of chips of translucent yellow PDM have almost no  $\text{Fe}_2\text{O}_3$  (column 1 in Table 2). Yellow PDM from the single nodule Windellama 13 has up to 10% silica, whereas other low-Fe PDM typically has ~1% silica.

**Table 3.** Average composition of three EMP analyses of Fe-poor PDM.

$\text{Al}_2\text{O}_3$	67.3
$\text{SiO}_2$	8.4
$\text{TiO}_2$	0.0
$\text{Fe}_2\text{O}_3$	2.0
Total	79.2

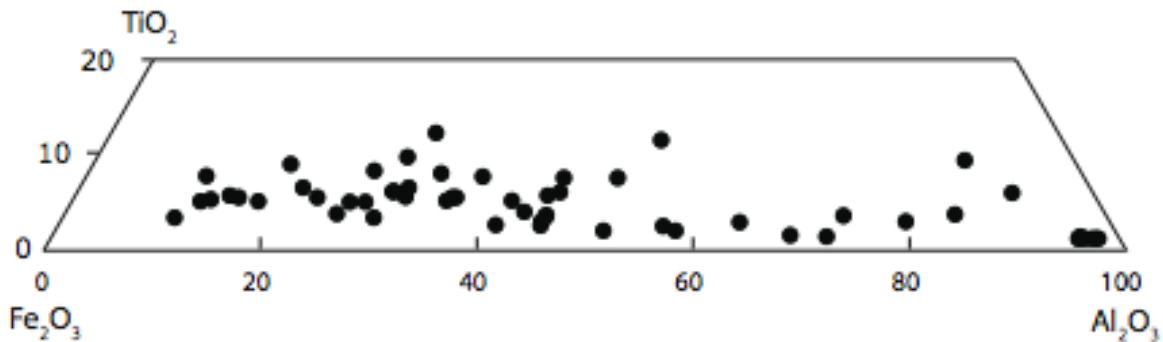


**Fig 5.** Composition triangle for Southern Highlands PDM,  $\text{SiO}_2$  neglected, recalculated to 100% ( $\text{Fe}_2\text{O}_3 + \text{Al}_2\text{O}_3 + \text{TiO}_2$ ).

### Discussion

The XRD and SEM results indicate that 20 nm crystals of hematite and maghemite occur as inclusions in a matrix of composition  $\text{Al}_2\text{O}_3$  with no more than 2 or 3%  $\text{Fe}_2\text{O}_3$ . The ubiquitous though small percentage of silica in PDM analyses may derive from primary kaolinite or halloysite, now altered to an unknown phase. TEM images of tubes 25-50 nm in diameter and of the order of 1  $\mu\text{m}$  in length have the size and morphology of halloysite observed in some bauxite samples.

Gibbsite with a grain size < 1  $\mu\text{m}$  converts to  $\chi$ -alumina on heating to around 470°C, whereas coarser gibbsite first transforms to boehmite and then to  $\gamma$ -alumina (Brindley & Choe 1960). Singh & Gilkes (1995) reported  $\chi$ -alumina in cracks in pisoliths from the Darling Range WA, and attributed it to recrystallization of an alumina gel. In burnt soils, maghemite is formed from iron oxyhydroxides at

temperatures below 450°C by reduction-oxidation (e.g. Fitzpatrick 1985, Ketterings *et al.* 2000, Grogan *et al.* 2003) or without reduction (Ye *et al.* 1998).

We surmise that bauxite pisoliths and nodules composed of fine-grained gibbsite and goethite rapidly lose water when heated by a burning tree root or stump, converting to a porous aggregate of  $\chi$ -alumina and iron oxide crystals. The phases that are, or most probably are present in PDM indicate the bauxite was heated to temperatures of around 450°C. Temperatures much beyond 500°C are precluded by the absence of higher temperature polymorphs of alumina and by the presence of maghemite, which converts to hematite above 500°C (Sidhu, 1988). The Southern Highlands surface exposures of bauxite are dominated by PDM. Any interpretation of the origin of these bauxites must take into account the presence and provenance of abundant PDM-rich pisoliths and nodules.

### **References**

- Brindley G.W. & Choe J.O. 1961. Reaction series gibbsite– $\chi$ -alumina– $\kappa$ -alumina. *American Mineralogist* **46**, 771-785.
- Fitzpatrick R. W. 1985. Iron compounds as indicators of pedogenic processes: Examples from the southern hemisphere. In: Stucki J.W., Goodman, B.A. & Schwertmann, U. eds. *Iron in soils and clay minerals*. NATO ASI Series C: Mathematical and Physical Sciences. 217; Pages 351-396.
- Grogan K.L., Gilkes R.J. & Lottermoser B.G. 2003. Maghemite formation in burnt plant litter at East Trinity, north Queensland, Australia. *Clays and Clay Minerals* **51**, 390-396.
- Ketterings Q.M., Bigham J.M. & Laperche V. 2000. Changes in Soil Mineralogy and Texture by Slash-and-Burn Fires in Sumatra, Indonesia. *Soil Science Society of America Journal* **64**, 1108-1117.
- Owen, H, B. 1954. Bauxite in Australia. Australian Bureau of Mineral resources, Geology and Geophysics, Bulletin 24. 234pp.
- Sidhu P.S. 1988 Transformation of trace-element substituted maghemite to hematite. *Clays and Clay Minerals* **36**, 31-38.
- Singh, B & Gilkes, R.J. (1995) The natural occurrence of  $\chi$ -alumina in lateritic pisolites. *Clay Minerals* **30**, 39-44.
- Ye, X., Lin, D., Jiaoz, Z. & Zhang, L. 1998. The thermal stability of nanocrystalline maghemite Fe<sub>2</sub>O<sub>3</sub>. *Journal of Physics D: Applied Physics* **31**, 2739-2744.

**Notes**